

Michael J. Murtagh
 Brookhaven National Laboratory
 Upton, New York 11973 USA

Introduction

The first observation of multileptons in high energy neutrino-nucleon interactions was reported¹ at the London Conference in 1974. Since then, the reported number of opposite sign dileptons has increased to a little more than a thousand and the predominant source for these events has been demonstrated to be the semileptonic decay of charmed particles. In the past year there has been a considerable amount of new data on this topic. Consequently, the emphasis here with regard to opposite sign dileptons will not be on establishing their origin but rather on the extent to which the new data expands on our knowledge of charm production in neutrino interactions.

The first reported observation of trileptons was in 1976.² In spite of some early hope that these events might be a signature for some new process, it is now agreed that the present data can be explained in terms of conventional mechanisms. No significant new data has recently become available on this topic. However, for completeness, a brief review of the present status will be given (Section 3).

The situation with regard to same sign dileptons is still not clear. New data from a number of experiments has recently become available. While all experiments have indications of a signal (Section 4), none is statistically significant. It is expected that a same sign dilepton signal will be a consequence of associated charm production. However there is no evidence from the one bubble chamber experiment reporting a signal for this process for the excess of strange particles one would expect from associated charm production.

Opposite Sign Dileptons

Theoretical Expectations

In the standard GIM³ model there are two allowed quark transitions for the production of single charmed particles in charged current neutrino interactions. One is the Cabbibo suppressed transition from the valence d-quark to the charmed c-quark.

$$(a) \quad \nu d \rightarrow \mu^- \bar{c} \\ \quad \quad \quad \downarrow \ell^+ \nu_s$$

Since a charm (not anti-charm) quark is produced, the semileptonic decay will yield a positive lepton and a hadron state with strangeness -1. The main features of this charm production mechanism are that the rate R_a is proportional to $D \sin^2 \theta_c$ where D is the down quark content in the nucleon, the x-distribution is a valence distribution, and there is one strange particle in each event. The other allowed transition is from an s-quark in the sea to a charm quark.

$$(b) \quad \nu s \bar{s} \rightarrow \mu^- \bar{c} \\ \quad \quad \quad \downarrow \ell^+ \nu_s$$

Here there is no Cabbibo suppression; the rate R_b is proportional to $S \cos^2 \theta_c$ where S is the strange quark content of the nucleon, the x-distribution will be a "sea" distribution and because of the presence of the spectator \bar{s} -quark, there should be two strange particles per event.

Two consequences of these allowed transitions are worth noting. Since the transition from the

valence quark is Cabbibo suppressed, one might expect both mechanisms to contribute significantly to the total charm production. In addition, the strange hadron always comes from the charm particle decay. Consequently if one observes an excess of Λ 's in opposite sign dileptons, this must arise from the decay of charmed baryons.

The principal features then of charm production in neutrino interactions are

- 1) the rate $R_\nu \propto D \sin^2 \theta_c + S \cos^2 \theta_c$ should be on the order of 10% of normal charged current interactions;
- 2) the x-distribution will be neither dominantly valence or sea, but some significant mixture of the two;
- 3) the strange particle content will be correlated with the relative S and D contributions to the x-distributions. Thus, if $\alpha_s = S/D$, the expected number of strange particles per event will be $(1 + \alpha_s)$.

The situation for anti-neutrinos is quite different. Again there are two allowed transitions

$$(a) \quad \bar{\nu} d \rightarrow \mu^+ \bar{c} \\ \quad \quad \quad \downarrow \bar{\nu} e^- \bar{s} \\ (b) \quad \bar{\nu} s \bar{s} \rightarrow \mu^+ \bar{c} \\ \quad \quad \quad \downarrow \bar{\nu} e^- \bar{s}.$$

In this case both transitions are from sea-quarks and since (a) is Cabbibo suppressed one can neglect it, to first order. Consequently one expects a rate $R_{\bar{\nu}} \propto S \cos^2 \theta_c$, a sea x-distribution and two strange particles per event.

It should be noted that unlike normal charged current interactions, the y-distribution for both neutrino and antineutrino production of charm is flat.

Rates for Dilepton Production by Neutrinos

There are now more than a dozen experiments reporting results on neutrino production of opposite sign dileptons. The majority of the events are from three counter experiments (Table I). All the experiments have data in high energy beams ($\langle E \rangle \gtrsim 70$ GeV), similar muon cuts and backgrounds. The bubble chamber data (Table II) is still dominated by the Brookhaven National Laboratory-Columbia University (BNL-COL) experiment although there is significant new data from two recent experiments (E546 from FNAL and WA14, the Gargamelle SPS group at CERN). Most of the bubble chamber data were obtained from lower energy neutrino beams ($\langle E \rangle \sim 30$ GeV) and, since in general the identified lepton pair was $\mu^- e^+$, the momentum cut on the positive track is low and the background less or comparable to the counter experiments. A notable exception here is the recent BFHSW experiment at FNAL which used the high energy Quad Triplet beam.

The raw measured production rate for $\mu^- \ell^+$ relative to the normal charged cut rate is quite sensitive to the beam used and the cuts employed by the various experiments. For example in Fig. 1 the momentum distributions for the μ^- and e^+ in the BC experiment are shown. Since the muon distribution is very broad, and

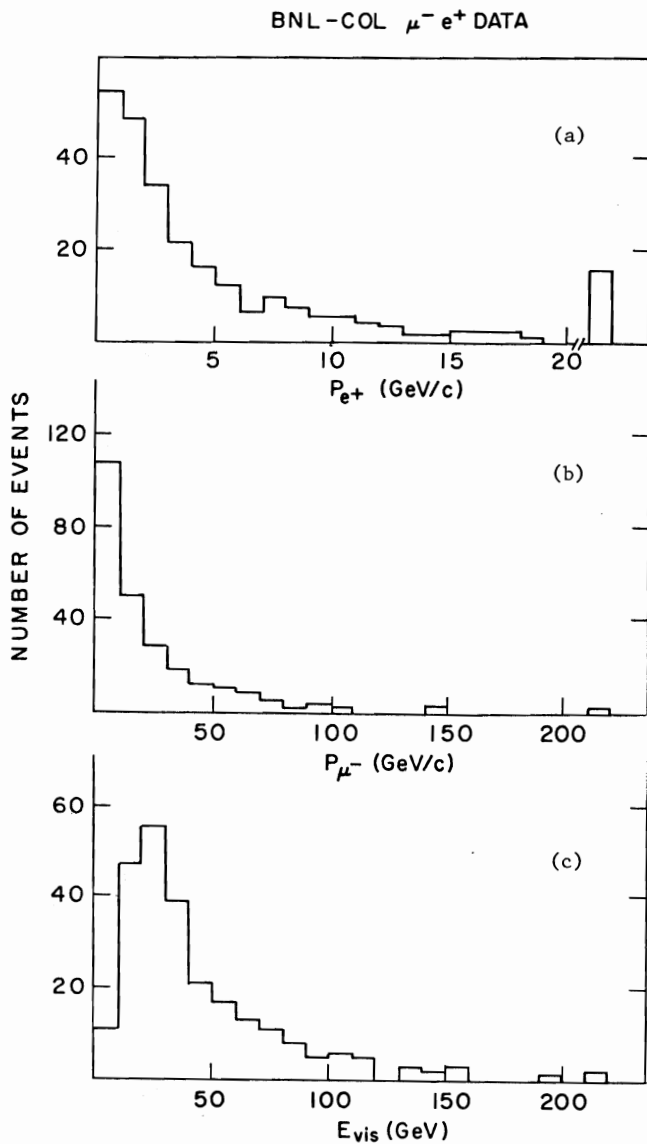


Figure 1. Distribution in a) positron momentum P_{e^+} , b) muon momentum P_{μ^-} , and c) the total visible energy E_{vis} for the $\mu^- e^+$ events in the BNL-COL experiment.

quite similar to the one from normal charged current interaction, a few GeV cut (~ 4 GeV) has little effect on the relative rate. However, a 4 GeV cut on the positron removes more than half the events and severely distorts the rate. This can be seen in Fig. 2 where the BC data with and without cuts is shown. The curve (Fig. 2) is taken from a charm production cross section calculation of Lai.¹⁸ While it is systematically lower than the uncut data points, the general shape is reproduced. The BC rate is in good agreement with that from other experiments. In Fig. 3 the rates for the bubble chamber experiments are compared. Within the rather poor statistics there is no disagreement. A more interesting comparison (Fig. 4) is of the BC data with 4 GeV cuts on the leptons and the counter experiments. The agreement, again, is remarkably good. Clearly all the ν -experiments are in agreement and Fig. 2 represents the first measurement of the excitation curve for charm production. A much better measurement with improved statistics might soon be expected. However there are problems in doing this. First, the bubble chamber since it has lower cuts is suited to measuring the low energy part of the distribution. However it is

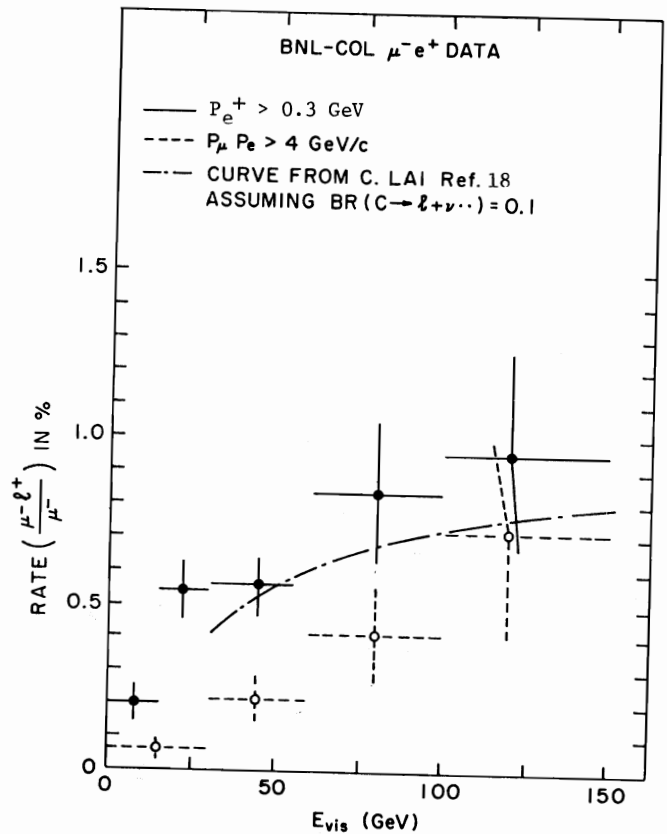


Figure 2. Ratio of the production cross sections for $\mu^- e^+$ events and charged current events as a function of measured neutrino energy. The data points are from the BNL-COL experiment. The curve is from a charm production calculation by C. Lai (Ref. 18).

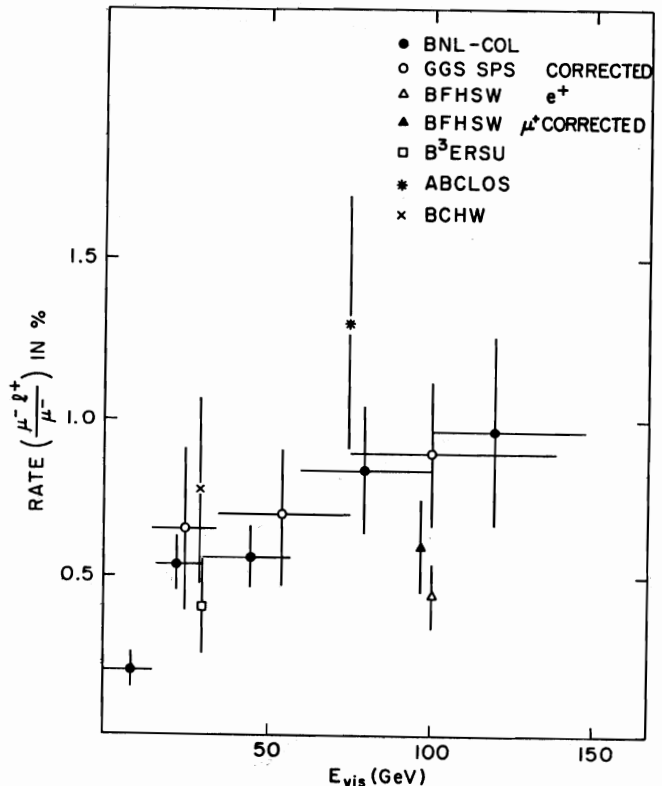


Figure 3. Comparison of bubble chamber measurements of the ratio of the production cross sections for $\mu^- e^+$ events and charged current events as a function of measured neutrino energy.

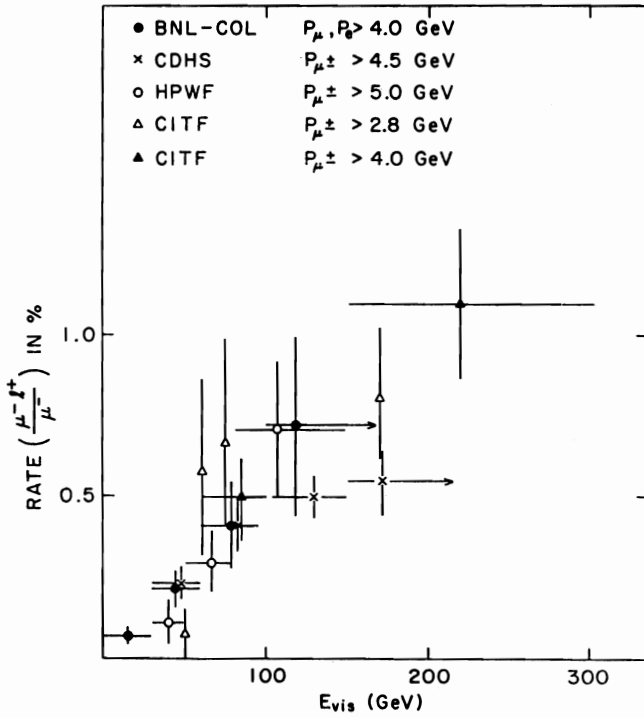


Figure 4. Comparison of counter experiment and BNL-COL experiment measurements of the ratio of the production cross sections for μ^+e^- events and charged current events as a function of measured neutrino energy.

unlikely that significant new bubble chamber data will be available for a least a couple of years. Secondly, counter experiments have superior statistics and higher energy cuts so they have greater problems with corrections for the z-distribution and missing neutrino energy. Neither of these quantities are well understood and are further confused by the unknown relative proportions of charmed baryons and charmed mesons produced in neutrino interactions.

Rates for Dilepton Production by Antineutrinos

There is still remarkably little information on dilepton production by antineutrinos (Tables III, IV). With the current statistics the production rate as measured by the various experiments is consistent with that expected from Lai's calculation (Fig. 5).

The relative rates for neutrino and antineutrino production of dileptons are comparable. This directly relates to the s-quark content of the nucleon as is discussed below.

Determination of the S-quark Content of the Nucleon

The fraction of S-quark in the nucleon can be determined in two independent ways. Since the y-distribution is the same both for dilepton production by neutrinos and antineutrinos, the ratio of the rates (R) is given by

$$R = \frac{R_V^-}{R_V^+} = \frac{\bar{S} \cos^2 \theta_c}{D \sin^2 \theta_c + S \cos^2 \theta_c}$$

or

$$\eta = \tan^2 \theta_c \frac{R}{1-R}$$

where $S \equiv \bar{S}$ and $\eta = S/D$.

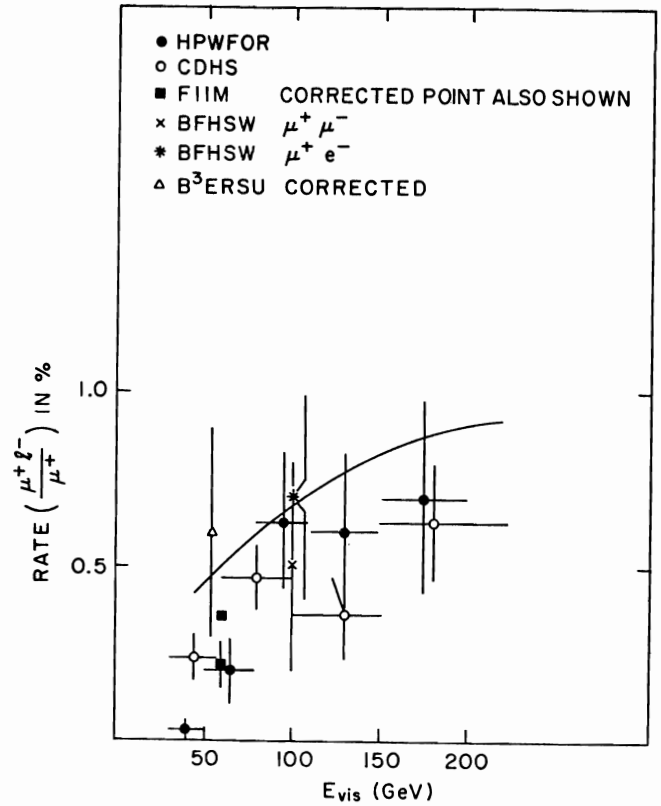


Figure 5. Ratio of the production cross section for μ^+e^- events and charged current events as a function of measured antineutrino energy. The curve is from a charm production calculation by C. Lai (Ref. 18) assuming a 10% charm semi-leptonic branching ratio.

Alternatively, since the antineutrino production is almost entirely off the s-quark, one can use the μ^+e^- data to determine the shape of the x-distribution for s-quarks. Then with a knowledge of the shape of the d-quark distribution from charged current data, one can fit the neutrino distribution to $Dx(1+\alpha_s xS/D)$ and consequently determine α_s . There are two points to be noted in these analyzes. First, since one is dealing with the transition from a light to a heavy quark, the appropriate variable is not x but $\xi = x + M_C^2/2myE_\nu$, the slow rescaling variable.²⁰ In addition, normal scaling violations should be taken into account. This implies at a minimum that charged current data at the same mean Q^2 as the dilepton rate should be used. Most recent analyzes incorporate both of these features. In Table V the current value for S/D are listed together with the method employed to extract them. The present quality of these measurements is illustrated in Fig. 6 where the preliminary results from the CDHS group on x-distribution is shown. The neutrino dilepton x-distribution is clearly narrower than the normal cc-distribution ($s = 0$ in the figure), and the antineutrino distribution fits $(1-\xi)^{10}$ which is to be compared to the $(1-\xi)^8$ distribution obtained from the antiquark content in cc-interactions. The agreement between all the experiments is good. It should be noted that α_s in the range of 2% to 6% corresponds to an expected strange particle content of between 1.3 and 1.6 strange particles per event in neutrino produced dilepton events.

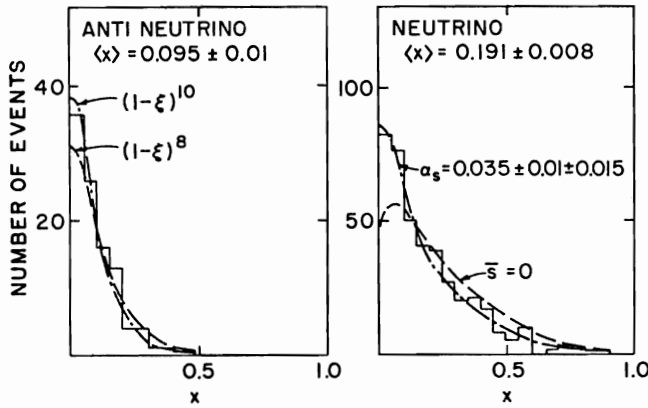


Figure 6. Distribution in x for neutrino and antineutrino opposite sign dilepton events for the CDHS data in Ref. 5b. The dot-dashed curves (---) are the best fits to the data for the appropriate mixture of valence and sea x -distributions. The dashed curves (---) represents the measured distributions in charged current interactions.

Strange Particle Production in μ^-e^+ Dilepton Events

The observed number of V^0 's ($K \rightarrow \pi^+\pi^-$, $\Lambda \rightarrow p\pi^-$) per μ^-e^+ event is listed in Table II and plotted in Fig. 7. More than half the events come from the BNL-COL experiment and the agreement between this experiment and the combined other data is shown in Table VI. The remainder of this section will discuss the analysis of the BNL-COL data and, where appropriate, the results will be compared with other experiments.

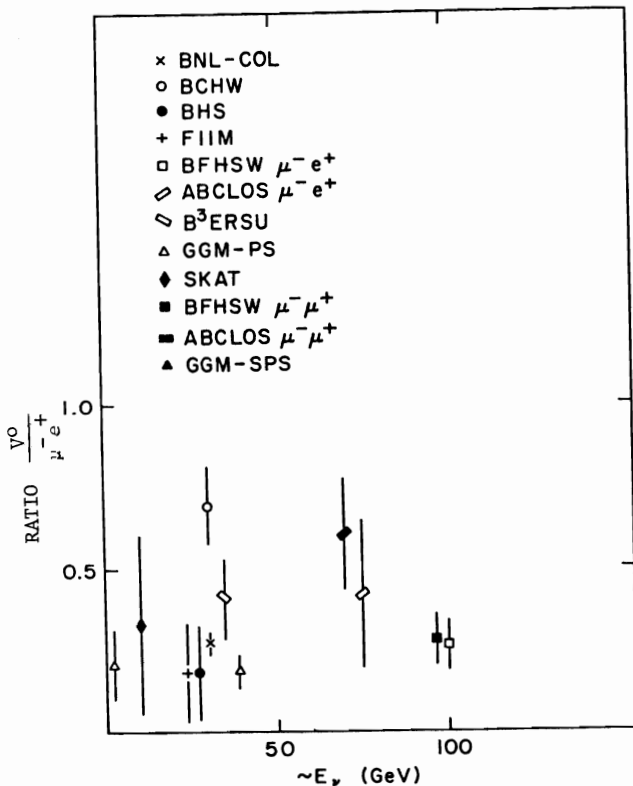


Figure 7. The observed V^0 content of μ^-e^+ events for the various bubble chamber experiments listed in Table II.

The observed dilepton V^0 rate of 0.27 ± 0.03 is clearly in excess of the normal charged current rate of 7% as is expected from charm production. After resolving K_s/Λ ambiguities the observed V^0 's break down to $37K_s$, 2Λ and $1\bar{\Lambda}$. There is no strong variation of the Λ or K^0 content with the energy of the events (Fig. 8).

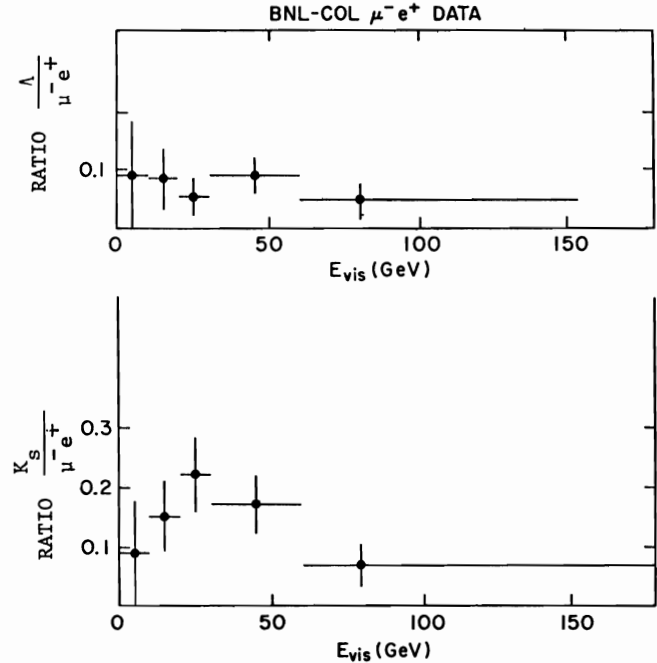


Figure 8. The observed a) Λ , b) K_s content of μ^-e^+ events as a function of E_{vis} . The data is from the BNL-COL experiment.

The excess over the number of strange particles expected in charged current interactions is $28 K_s$, 13Λ , $0 \bar{\Lambda}$. After correcting for neutral decay modes and detection efficiencies there are $101 \pm 25 \bar{K}^0$ and $23 \pm 9 \Lambda$ or an excess of 0.6 ± 0.15 neutral strange particles per μ^-e^+ event. Consequently, if charged and neutral strange particles are equally produced the number of strange particles per μ^-e^+ event is ~ 1.2 per event. This is in reasonable agreement with the expectations from the s -quark content in the nucleon discussed previously. It should be noted that

$$\frac{\text{No. of } \mu^-e^+ \Lambda \dots}{\text{No. of } \mu^-e^+ K^0 \dots} = 0.23 \pm 0.1.$$

This relates to the relative amounts of charmed baryon and charmed meson production in neutrino interactions. However at present it is difficult to interpret because the charmed baryon decay modes are not well measured ($\Lambda_c^+ \rightarrow \Lambda \dots \Lambda_c^+ \rightarrow K^0 = ?$) and the semi-leptonic decay rates of the D -mesons and charmed baryons are not understood.

The $K_s e^+$ effective mass distribution is shown in Fig. 9a and for a combination of other experiments in Fig. 9b. The data (Fig. 9a) is very consistent with a four-body decay of the D -mesons. It is not possible to distinguish between $K^* e \nu$ and $K \pi e \nu$ decays. A purely three-body decay is not consistent with the data. However this is not surprising since only the D^+ 3-body decay ($D^+ \rightarrow K_s e^+ \nu$) can contribute to the plot ($D^0 \rightarrow K^+ e^+ \nu$ has no K_s) while both D^0 , D^+ 4-body decays contribute. While the $K_s e^+$ mass distribution is very consistent with

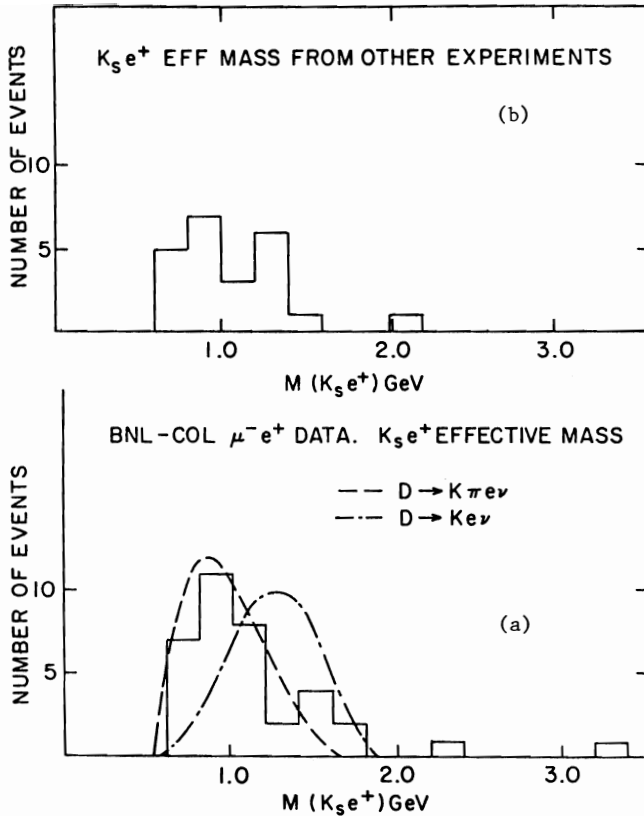


Figure 9. The $K_s e^+$ effective mass distribution in the reaction $\nu + N \rightarrow \mu^- + e^+ + K_s + \dots$ for a) the BNL-COL experiment; b) other experiments.

that expected from D-meson decays it is worth noting that it is probably not inconsistent with some charmed baryon decays ($\Lambda_c^+ \rightarrow K_s e^+ \nu$ for example).

The Λe^+ effective mass distribution is shown in Fig. 10a. Since 20 Λ 's are observed and only 7 are expected from normal charged current associated production, there is a significant excess of Λ production. As discussed earlier this implies the existence of charmed baryon production in neutrino interactions. One important feature in Fig. 9b is that almost all the events with $P_{e^+} > 4$ GeV have effective masses larger than the Λ_c^+ . This implies that the electron spectrum from charmed baryon decays may be softer than that for meson decays. This point was first noticed in the dilepton bubble chamber experiments^{15,16} where there is a high momentum cut ($P_{e^+} \gtrsim 4$ GeV) and where no excess Λ production was observed (Fig. 10b). This result clearly has implications for counter experiments trying to correct for the effect of their momenta cuts to determine the charm production rate.

Strange Particle Production in $\bar{\nu}$ Interactions

The observed numbers of V^0 's are listed in Table IV. There are large fluctuations in the rather small data samples available so it is perhaps best to use only the average value for V^0/μ^+e^- of 0.48 ± 0.08 . This is higher than the observed rate for neutrinos

$$\frac{(\bar{\nu} \rightarrow \mu^+ e^- V^0)}{(\bar{\nu} \rightarrow \mu^+ e^-)} \bigg/ \frac{(\nu \rightarrow \mu^- e^+ V^0)}{(\nu \rightarrow \mu^- e^+)} = 1.7 \pm 0.3.$$

If one assumes the relative corrections for anti-neutrinos are the same as those for neutrinos, this converts to a neutral strange particle rate of 1.02 per event (0.6×1.7) or ~ 2 strange particles per event as

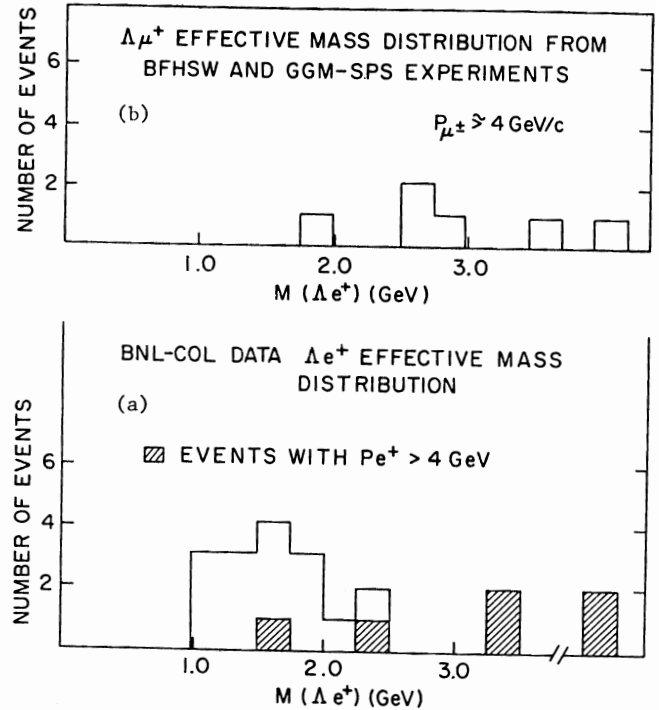


Figure 10. The Λe^+ effective mass distribution in the reaction $\nu N \rightarrow \mu^- \Lambda^+ \Lambda^0 + \dots$ for a) the BNL-COL experiment; b) the BFHSW and BCCEMO experiments.

expected in the GIM model. Clearly additional data is required to properly establish this conclusion.

Trilepton Production

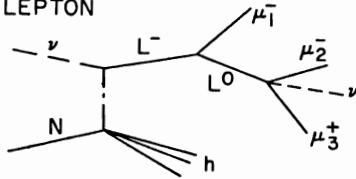
Neutrino events with 3μ in the final state were first reported by the CITF group² in 1976. Shortly afterwards they were observed by the HPWFOR group²² also at FNAL and later by the CDHS group²³ at the CERN SPS. Many possible origins for these events were proposed²⁴ and some early results suggested new heavy leptons as a significant source. Recently much larger data samples (Table VII) from the CDHS²⁵ and HPWFOR²⁶ groups have allowed a more detailed analysis of the origin of these events. The results from both analyses are in very good agreement. Recently the CDHS group reported the observation of 8 antineutrino produced trilepton events ($\bar{\nu} \rightarrow \mu^+ \mu^- \mu^+$). The properties of these events are such that their origin can be understood in terms of the same mechanisms used to explain the neutrino production of trileptons.²⁸ However much larger statistics are required to give an independent analysis.

The most likely sources of trileptons (Fig. 11) are the production of new objects such as heavy leptons or heavy quarks or conventional processes such as electromagnetic muon pair production or hadronic muon pair production. Present analyses indicate that the current data can be satisfactorily understood in terms of these conventional mechanisms. However it should be noted that the limits on the production of heavy quarks or leptons are not very restrictive. The muon pair production processes are characterized by low effective masses for the secondary muons (M_{23}) and the amount of electromagnetic muon pair production can be estimated from the number of events in which the secondary muon pair is correlated in angle ($\phi_{1,2+3} \simeq 0$) with the leading muon.

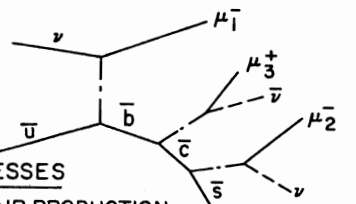
SOURCES OF TRILEPTONS

NEW OBJECTS

a) NEW HEAVY LEPTON

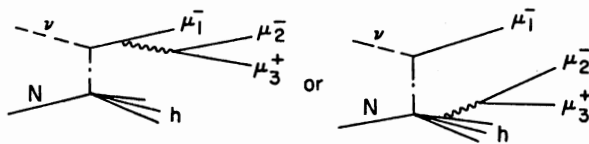


b) NEW HEAVY QUARK



NORMAL PROCESSES

c) EL. MAG μ-PAIR PRODUCTION



d) HADRONIC μ-PAIR PRODUCTION

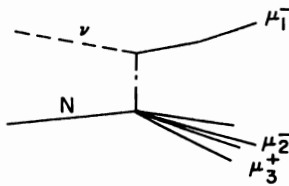


Figure 11. Possible sources for triplepton events
 a) Heavy lepton cascade; b) Heavy quark cascade; c) Electromagnetic muon pair production; d) Hadronic muon pair production.

The rate for triplepton production as a function of neutrino energy is shown in Fig. 12. The rapid rise is largely due to reduced acceptance at low energy caused by the high muon momentum cuts.²⁵ The azimuthal angle $\phi_{1,2+3}$ (Fig. 13) between the projection onto the plane normal to the nominal neutrino direction of the leading muon (μ_1) and the sum of the secondary muons ($\mu_2 + \mu_3$) is shown in Fig. 14 for the CDHS data. The strong backward peaking indicates that the triplepton production is largely associated with the hadronic vertex. However there is a slight peaking in the forward direction suggesting muon pair production associated with the leading muon as expected from electromagnetic production. As shown in the figure the data can be well reproduced by the conventional mechanisms. The effective mass (M_{23}) of the secondary muons is shown in Fig. 15 for the CDHS data. It peaks at very low mass (< 1 GeV) which is very consistent with conventional μ -pair production and not in agreement with the expectations from new heavy objects. From Fig. 15 the 90% confidence limit for \bar{b} production (for events with $E_\nu > 30$ GeV) is that less than 10% of the observed triplepton events could come from this source. It might appear that Fig. 15 can accommodate significant L^- production. It should be noted that the masses were chosen ($M_{L^-} = 9$ GeV, $M_{L^0} = 1.5$ GeV) to give reasonable agreement with the effective mass distribution. However with these mass selections the predicted transverse momentum of the non-leading $\mu^-\mu^+$ pair with respect to the hadron direction are substantially larger than the observed transverse momentum Fig. 16. From this plot one concludes that at the 90% confidence level less than 17% of the observed trimuons come from

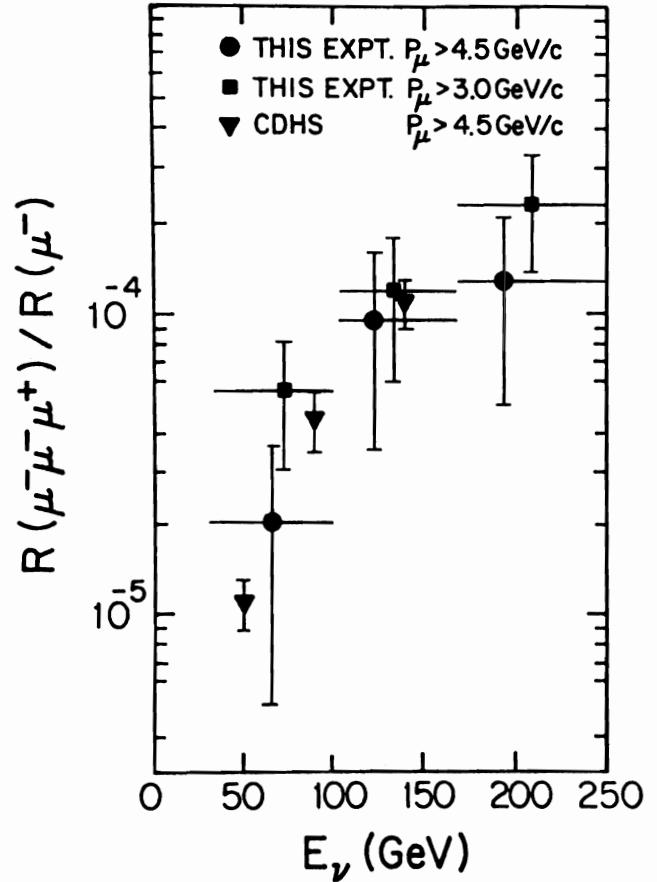


Figure 12. The trimuon rate relative to the neutrino charged current rate as a function of neutrino energy. CDHS is from Ref. 25, while this Exp. is HPWFOR from Ref. 26.

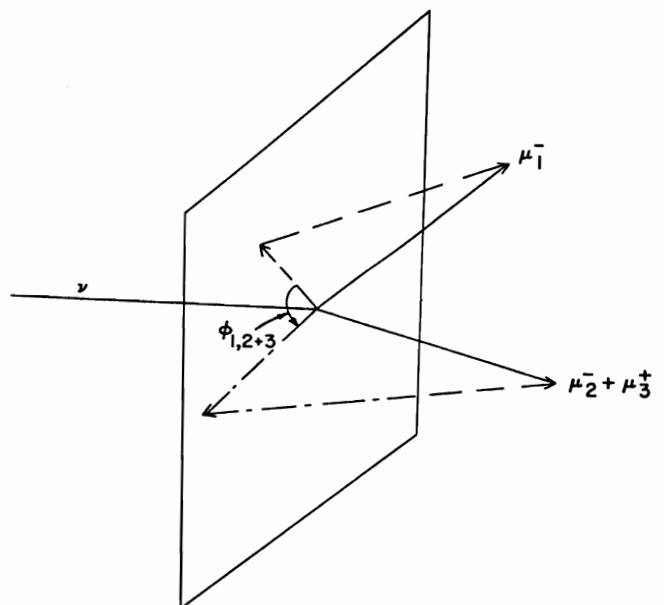


Figure 13. Definition of the azimuthal angle $\phi_{1,2+3}$.

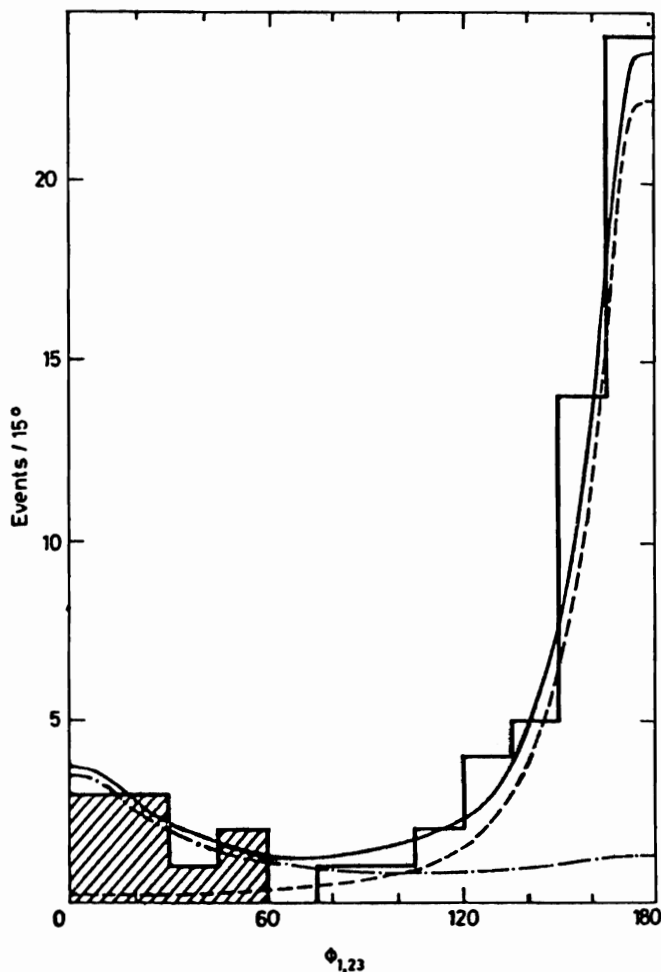


Figure 14. Azimuthal angle between the leading muon and the pair $\mu_2 + \mu_3$. The lines in the figure have the following meaning: dot-and-dash curve = internal bremsstrahlung, normalized to $\phi_{1,23} < 60^\circ$; dashed curve = hadronic pair production; full curve = sum of both. Data and curves are from CDHS exp. (Ref. 25).

L^- , L^0 production with the selected mass values. The CDHS trilepton events can, therefore, be interpreted as follows. Approximately 25% of the events (corresponding to a rate of $(0.8 \pm 0.4) \times 10^{-5}$ relative to single muon production) are due to electromagnetic muon pair production. The remaining 75% $((2.2 \pm 0.4) \times 10^{-5}$ relative to single muon production) are due to hadronic muon pair production. However the limits on the production of new objects are not very restrictive being in the range of 10 - 20% of the events.

Similar conclusions come from the analysis of the HPWFOR data, Fig. 17. The only difference here is that a 20% contribution from associated charm (cc) production is included and the hadronic muon-pair production reduced to compensate. The magnitude of the cc contribution to be included was determined from the group's observed rate for same sign dilepton production (see the following section).

It is perhaps worth noting that the present understanding of trilepton production in terms of conventional mechanisms simply implies that one can reproduce the shapes of the measured distributions using distributions from processes which ought to occur at roughly the observed level. (For example any hadronic μ -pair production mechanism which produces low mass pairs (e.g. vector meson production) will reproduce the shape of

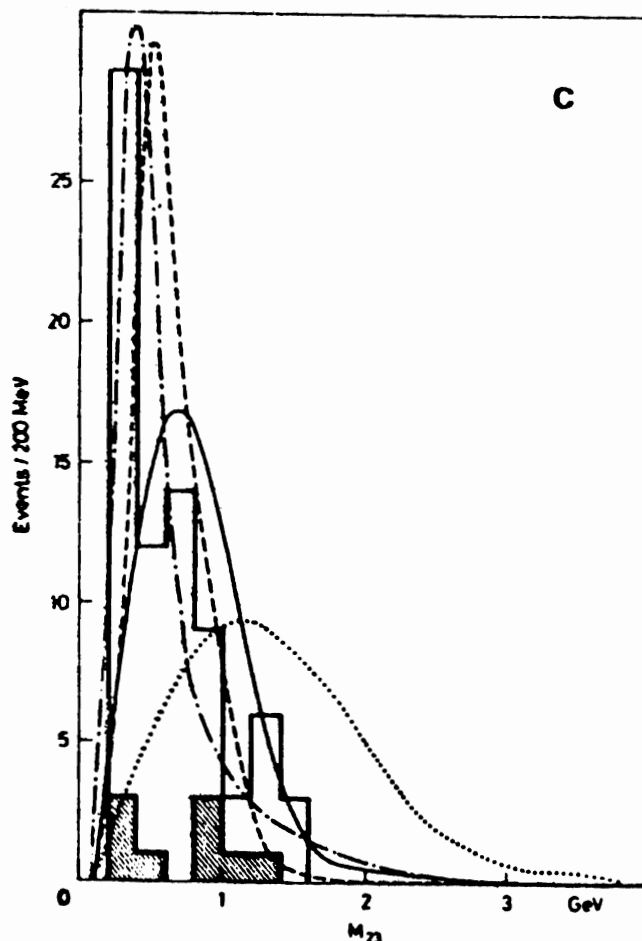


Figure 15. Dimuon (M_{23}) mass distribution. The lines have the following meaning: dashed curve = hadronic pair production; dot-and-dash curve = internal bremsstrahlung; full curve = heavy lepton cascade (L^-/L^0) = (9 GeV/1.5 GeV); dotted curve = heavy quark cascade. The predictions are normalized to the total number of events. The data and curves are from CDHS exp. (Ref. 25).

the hadronic component of the $\phi_{1,2+3}$ distribution). Detailed calculations presently yield rates ~ 2 times lower than the observed values.²⁹ Alternatively, since the trimuon acceptance peaks at large x , one can obtain good quantitative agreement with the observed rate by requiring a different x -dependence for the neutrino and pion muon pair production. This effect is suggested by the data.²⁵

Same Sign Dilepton Production

Over the past few years as has been discussed earlier a number of groups have reported the observation of opposite-sign dileptons at $\sim 1\%$ of the normal charged current rate. These events can be understood as the production and semi-leptonic decay of charm particles. The dominant backgrounds which come from π and K decay are typically ~ 10 -20% of the signal or $\sim 10^{-3}$ of normal charged current interactions. However, the search for same-sign dileptons ($\nu \rightarrow \mu^- \ell^-$) is still a major experimental problem. The difficulty here is that π and K decays contribute at approximately the same level as the expected $\mu^- \ell^-$ signals. Consequently, a detailed understanding of the background is critical in this case. The first reported signal for this process was from the HPWFOR group at FNAL.³⁰ Since their detector contained two different density targets the production rates in the two targets as a function of the muon

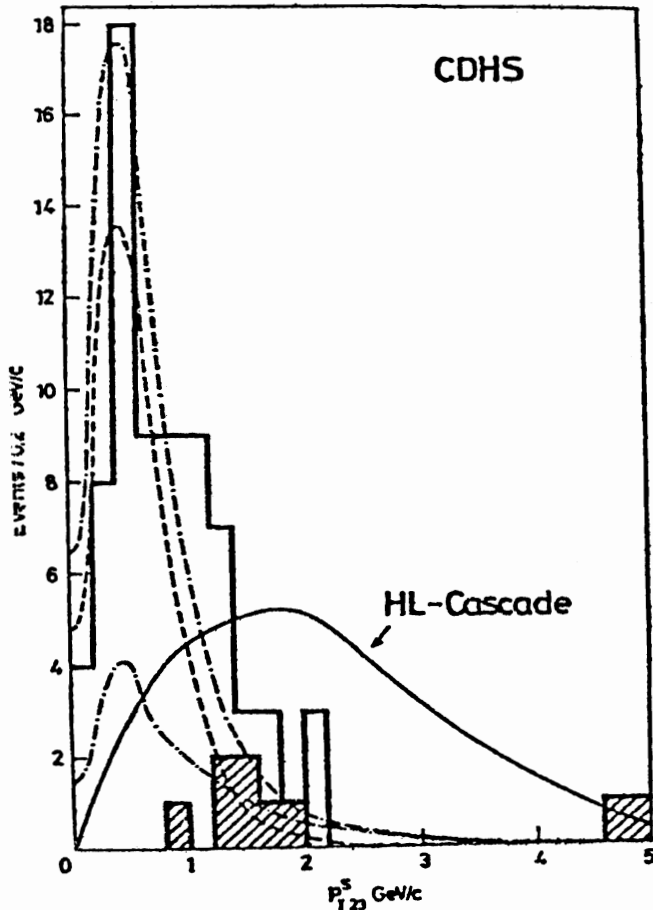


Figure 16. Transverse momentum distribution of $\mu_2 + \mu_3$ with respect to the hadron shower direction. The lines have the same meaning as in Fig. 14. Data and curves are from CDHS experiment (Ref. 25).

energy cut could be used both to check the validity of the Monte Carlo background calculations and to extrapolate to infinite density to obtain a prompt $\mu^- \ell^-$ signal. Unfortunately, the statistics in this experiment are rather small and their final result for a 10 GeV muon cut was a rate $(12 \pm 5)\%$ relative to opposite sign dileptons, a 2-3 σ effect. In the past few months a number of other measurements for this process have been reported (Table VIII). This includes improved statistics from the CDHS group and the first bubble chamber measurement from the BNL-COL group. In general because of variations in acceptance corrections the experimental measurements are compared relative to opposite-sign dilepton production. Within the present statistics and allowing for different mean neutrino beam energies the results are consistent. In all cases the significance is $\sim 2 - 3\sigma$ and the rates $\sim 5\%$ with 10 GeV muon and electron cuts. Since the opposite sign dilepton rate is $\sim 1\%$ this corresponds to a rate for same-sign dileptons of $\sim 10^{-4} - 10^{-5}$ of normal charged current events.

One possible source for same-sign dileptons is fed down from trileptons where the μ^+ of the trilepton is below the muon energy cut. However, this source cannot produce a signal at the presently observed level.³² A more likely candidate for same-sign dilepton production is associated charm production where the \bar{c} decays semileptonically ($\nu + \mu^- cc \rightarrow \mu^- ss \ell^- \nu \dots$). This model can reproduce the features of the distributions observed,³³ but it should be noted that present models for this mechanism yield rates on the order 10^{-6} of charged current event and not 10^{-4} . If one is seeing associated charm production then there should be an excess of

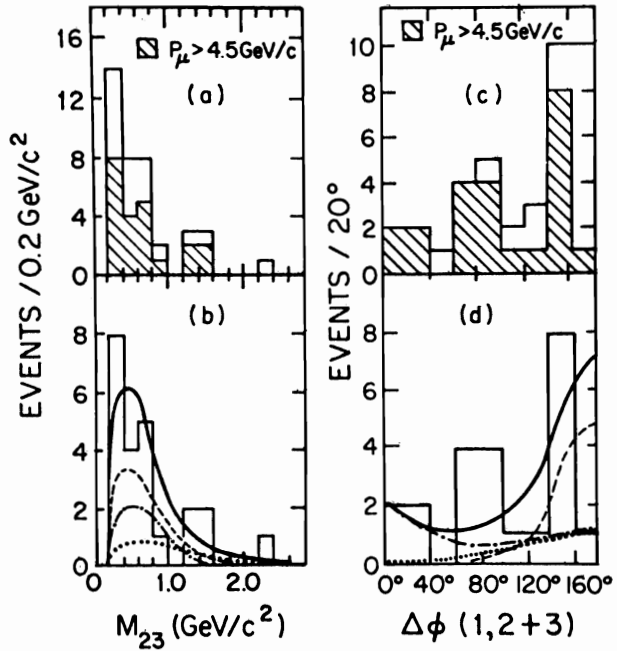


Figure 17. a) The mass of the muon pair for $p_\mu > 3.0$ and 4.5 GeV/c . b) The mass for $p_\mu > 4.5 \text{ GeV/c}$. Dash-dotted curve; radiative pairs; dashed curve, direct pairs; dotted curve, charm-anticharm production; and solid curve, total. c) The azimuthal angular difference ($\Delta\phi$) between the leading muon and the pair. d) The $\Delta\phi$ distribution for $p_\mu > 4.5 \text{ GeV/c}$. The curves are as in (b). Data and curves for the HPWFOR exp. (Ref. 26).

strange particle production since both the c and \bar{c} will decay to strange particles. More precisely in the 20 $\mu^- e^-$ bubble chamber events (11 $\mu^- e^-$ above background) one would expect to observe between 4 and 5 V^0 's ($K_S^0 \rightarrow \pi^+ \pi^-, \Lambda \rightarrow p \pi^-$) depending on the relative amounts of Λ_c and $D\bar{D}$ produced. (It is also assumed that the charmed particles decay equally to charged and neutral strange particles.) In the 20 $\mu^- e^-$ candidates only one V^0 (a $K_S^0 \rightarrow \pi^+ \pi^-$) is observed. While this is not inconsistent with the expected 4-5 V^0 's there is clearly no observed excess such as one might have expected.

The situation with regard to same-sign dileptons therefore is still unclear. A number of experiments have reported 2-3 σ level signals but none is conclusive. If one considers this combination of signals from independent experiments to be a significant measure of $\mu^- e^-$ production then the one bubble chamber experiment which has a signal at the appropriate level has no evidence for the excess strange particle production one would expect from cc production.

Conclusion

The new data accumulated over the past year on multilepton production in neutrino interactions has improved our understanding of the basic processes involved. There is good agreement among the various experiments on all topics. However, it is also apparent that better statistics are required in many instances. This is particularly true for antineutrino bubble chamber experiments.

The opposite sign dilepton events are clearly consistent with being predominantly single charm production. There is now evidence in this data for charm baryon as well as charm meson production. However it

is not yet possible to measure the relative amounts of charm mesons and charm baryon produced. There is general agreement that the present trilepton data can be qualitatively understood in terms of muon pair production processes. However it appears difficult to get satisfactory quantitative agreement with the data. It is likely that with improved statistics and with additional data from pion and the new muon experiments on multilepton production that good quantitative agreement will be obtained in the not too distant future. On the other hand, it should be remembered that the present limits on new particle production are not very restrictive. Consequently, it is certainly possible that improved statistics will produce more interesting physics.

Perhaps the most interesting recent data has been on same sign dilepton production. Since there should be associate charm production in neutrino interactions, there should be same sign dilepton events. At present there are indications of a signal from all the counter experiments and the one bubble chamber experiment with reasonable statistics. However none of the signals are statistically significant and there is no obvious excess of strange particles such as would be expected from associated charm production.

References

1. C. Rubbia, Proc. of the 17th International Conf. on High Energy Physics, London 1974, PIV-117.
2. B.C. Barish et al., Phys. Rev. Lett. 38 (1977) 577.
3. S.L. Glashow, J. Iliopoulos, L. Maiani, Phys. Rev. D2 (1970) 1285.
4. A. Benvenuti et al., Phys. Rev. Lett. 34 (1975) 419; and 41 (1978) 1204; A.K. Mann, Proc. of the XIV Rencontre de Moriond, 1979.
5. M. Holder et al., Phys. Lett. 69B (1977) 377; and H.J. Willutzki, Proc. of Neutrino 79 Conf., Bergen, Norway, 1979.
6. B.C. Barish et al., Phys. Rev. Lett. 36 (1976) 939; and D. Buchholz, Proc. of the 19th Int'l. Conf. on High Energy Physics, Tokyo, 1978, p. 332; and K. Nishikawa et al., Univ. of Rochester preprint UR-711 (1979).
7. H. Deden et al., Phys. Lett. 67B (1977) 474.
8. P. Bosetti et al., Phys. Rev. Lett. 38 (1977) 1248.
9. C. Baltay et al., Phys. Rev. Lett. 39 (1977) 62.
10. H.C. Ballagh et al., Phys. Rev. Lett. 39 (1977) 1650.
11. C.T. Murphy et al., Proc. XIth Rencontre de Moriond, 1977, p. 301.
12. P.C. Bosetti et al., Phys. Lett. 73B (1978) 380.
13. O. Erriquez et al., Phys. Lett. 77B (1979) 227.
14. J.P. Berge et al., Phys. Lett. 81B (1979) 89.
15. H.C. Ballagh et al., Univ. of Hawaii preprint UH-511-350-79, July 1979; and R.J. Loveless, Proc. of Neutrino 79 Conf., Bergen, Norway, 1979.
16. N. Armenise et al., CERN preprint CERN/EP/79-48.
17. D.S. Baranov et al., Phys. Lett. 81B (1979) 261.
18. C. Lai, Phys. Rev. D18 (1978) 1422.
19. N. Armenise et al., Proc. of Neutrino 79 Conf., Bergen, Norway, 1979.
20. R.M. Barnett, Phys. Rev. Lett. 36 (1976) 1163.
21. C. Matteuzzi, Proc. of Neutrino 79 Conf., Bergen, Norway, 1979.
22. A. Benvenuti et al., Phys. Rev. Lett. 38 (1977) 1110.
23. M. Holder et al., Phys. Lett. 70B (1977) 393.
24. C.H. Albright, J. Smith, J.A.M. Vermaseren, Phys. Rev. D18 (1978) 108 and refs. in this paper.
25. T. Hansl et al., Nucl. Phys. B142 (1978) 381.
26. A. Benvenuti et al., Phys. Rev. Lett. 42 (1979) 1024.
27. J.G.H. de Groot et al., Centre d'Etudes Nucleaires de Saclay preprint DPhPE79-06 (1979).
28. J. Smith, CERN preprint TH.2657-CERN(1979).
29. V. Barger, T. Gottschalk, R.J.N. Phillips, Phys. Rev. D18 (1978) 203.
30. A. Benvenuti et al., Phys. Rev. Lett. 41 (1978) 725.
31. M. Holder et al., Phys. Lett. 70B (1977) 396.
32. J.G.H. de Groot et al., Paper L-4 submitted to this Conf.
33. J. Smith, Proc. of Neutrino 79 Conf., Bergen, Norway, 1979.

This research supported by the U.S. Department of Energy.

Table I. Dilepton Production by Neutrinos in Counter Experiments

<u>Experiment</u>	<u>Beam</u>	E_ν <u>GeV</u>	<u>Events</u> <u>Observed</u>	<u>Cuts in GeV</u>	<u>Approximate</u> <u>Background in %</u>	$\mu^- \mu^+ / \mu^-$ <u>Rate in %</u>
Harvard/Penn/Wisconsin/ FNAL/Ohio/Rutgers ⁽⁴⁾	QuadTriplet (QT) Sign Selected Bare Target (SSBT)	100	199 $\mu^- \mu^+$	$P_\mu^\pm > 5$	25	.65 ± .13 $E_\nu > 80$ GeV
CERN/Dortmund/Heidelberg/ Saclay ⁽⁵⁾	NarrowBand Beam (NBB)	80	405 $\mu^- \mu^+$	$P_\mu^\pm > 4.5$	14	.46 ± 0.04
CIT/FNAL/Rochester/ Rockefeller/Northwestern ⁽⁶⁾	QT	100	203 $\mu^- \mu^+$	$P_\mu^\pm > 4$	15	~.66

Table II. Dilepton Production by Neutrinos in Bubble Chamber Experiments

Experiment	Beam	E_ν	Events Observed	Cuts in GeV	Back-ground %	$\mu^- \ell^+ / \mu^-$ Rate in %	V^0 (a)	$V^0 / \mu^- \ell^+$ (b) Rate in %
Gargamelle ⁽⁷⁾ CERN PS	WideBand Beam (WBB)	2	17 $\mu^- e^+$	$P_e^+ > 0.2$	33	0.31 \pm .13	3	.21 \pm .11
Berkeley/CERN/ Hawaii/Wisconsin ⁽⁸⁾ FNAL Exp. 28	WBB	30	17 $\mu^- e^+$	$P_{\mu^+}^- > 4$ $P_e^+ > 0.8$	5	0.77 \pm .3	11	.69 \pm .12
BNL/Columbia ⁽⁹⁾ FNAL Exp. 53A	WBB	30	249 $\mu^- e^+$	$P_e^+ > 0.3$	14	0.52 \pm .10	58	.27 \pm .03
Berkeley/Hawaii/ Seattle ⁽¹⁰⁾ FNAL Exp. 172	$\bar{\nu}$ WBB	30	6 $\mu^- e^+$	$P_{\mu^+}^\pm > 4$ $P_e^+ > 0.8$	15	0.34 $^{+.23}_{-.13}$	1	.18 \pm .16
FNAL/LBL/Hawaii ⁽¹¹⁾ FNAL Exp. 460	QT	100	9 $\mu^- \mu^+$	$P_{\mu^+}^\pm > 4$	33	--	1	.11 \pm .01
Aachen/Bonn/CERN/ London/Oxford/ Saclay ⁽¹²⁾ CERN SPS Exp. WA19 in BEBC	Narrow Band Beam (NBB)	80	10 $\mu^- \mu^+$ 5 $\mu^- e^+$	$P_{\mu^+}^\pm > 4$ $P_e^+ > 0.3$	30 6	0.8 \pm .3 0.7 \pm .3	5 2	.60 \pm .17 .42 \pm .23
Bari/Birmingham/ Brussels/Ecole Poly- technique/Rutherford/ Saclay/London ⁽¹³⁾ CERN SPS Exp. WA24 in BEBC	WBB	30	17 $\mu^- e^+$	$P_e^+ > 0.3$	14	0.41 \pm .15	6	.41 \pm .13
FNAL/Michigan/ IHEP/ITEP ⁽¹⁴⁾ FNAL Exp. 180	$\bar{\nu}$ WBB	30	6 $\mu^- e^+$	$P_{\mu^+}^\pm > 4$ $P_e^+ > 0.8$	15	1.9 \pm 1.0	1	.18 \pm .16
Berkeley/FNAL/ Hawaii/Seattle/ Wisconsin ⁽¹⁵⁾ FNAL Exp. 546	QT	100	54 $\mu^- \mu^+$ 29 $\mu^- e^+$	$P_{\mu^+}^\pm > 4.0$ $P_e^+ > 0.3$	33 6	0.37 \pm .10 0.44 \pm .10	10 7	.28 \pm .08 .26 \pm .08
Bari/CERN/Ecole Polytechnique/Milan/ Orsay ⁽¹⁶⁾ CERN SPS Exp. WA14 in GARGAMELLE	WBB	2	94 $\mu^- \mu^+$	$P_{\mu^+}^\pm > 2.6$	33	0.72 \pm .14	12	.19 \pm .05
SKAT ⁽¹⁷⁾ Serpukhov	WBB	10	3 $\nu^- e^+$	$P_e^+ > 0.5$	--	0.7 \pm .4	1	.33 \pm .27

a) $V^0 \equiv (K_s^+ \rightarrow \pi^+ \pi^+, \Lambda \rightarrow p \pi^-)$ b) Rate is corrected for $\mu^- \ell^+$ background

Table III. Dilepton Production by Antineutrinos in Counter Experiments

Experiment	Beam	Events	Cuts in GeV	Approximate Background in %	$\frac{\mu^+ \mu^-}{\mu^+}$ Rate in %
Harvard/Penn/Wisconsin/ FNAL/Ohio/Rutgers ⁽⁴⁾	SSBT	$49\mu^+ \mu^-$	$P_{\mu^{\pm}} > 5$	25	$.7 \pm .25$ $E_{\nu} > 80 \text{ GeV}$
CERN/Dortmund/ Heidelberg/Saclay ⁽⁵⁾	NBB	$101\mu^+ \mu^-$	$P_{\mu^{\pm}} > 4.5$	12	$.34 \pm 0.04$

Table IV. Dilepton Production by Antineutrinos in Bubble Chamber Experiments

Experiment	Beam	Events Observed	Cuts in GeV	Back-ground %	$\frac{\mu^+ e^-}{\mu^-}$ Rate in %	V^0 (a)	$V^0/\mu^+ e^-$ (b) Rate in %
Bari/Birmingham/ Brussels/Rutherford/ Saclay/London ⁽¹⁹⁾ CERN SPS Exp. WA24 BEBC with TST	WBB	$43\mu^+ \mu^-$	$P_{\mu^{\pm}} > 3$	33	$.6 \pm .3$	7	$.27 \pm .09$
Berkeley/FNAL/Hawaii/ Seattle/Wisconsin ⁽¹⁵⁾ FNAL Exp. 546	QT	$54\mu^+ \mu^-$ (c) $10\mu^+ e^-$	$P_{\mu^{\pm}} > 4$ $P_{e^-} > .8$	33 10	$.5 \pm .3$ $.7 \pm .3$	- 2	- $.40 \pm .22$
FNAL/Michigan/IHEP/ ITEP ⁽¹⁴⁾ FNAL Exp. 180	WBB	$12\mu^+ e^-$	$P_{\mu^{\pm}} > 4$ $P_{e^-} > .8$	16	$.22 \pm .07$	10	$1.0 \pm .05$
Berkeley/Hawaii/ Seattle ⁽¹⁰⁾ FNAL Exp. 172	WBB	$4\mu^+ e^-$	$P_{\mu^{\pm}} > 4$ $P_{e^-} > .8$	15	$.15^{+.14}_{-.08}$	2	$.67 \pm .29$
					TOTAL	21	$.48 \pm .08$

a) $V^0 \equiv (K_s^+ \rightarrow \pi^+ \pi^+, \Lambda \rightarrow p \pi^-)$

b) Rate is corrected for $\mu^+ e^-$ background

c) This is the sum of neutrino ($\nu \rightarrow \mu^+ \mu^-$) and antineutrino ($\bar{\nu} \rightarrow \mu^+ \mu^-$) dimuon events

Table V. Determination of S-quark Content

<u>Experiment</u>	<u>Method</u>	$\bar{S}/Q + \bar{Q}$
HPWFOR ^(4c)	Rate ($\bar{\nu}/\nu$)	.032 ± .015
CDHS ^(5b)	Rate	.031 ± .006 (±.005)
	X-Distribution	.035 ± .01 (±.015)
Gargamelle ⁽²¹⁾	X-Distribution	.021 ± .013
BEBC/Gargamelle ⁽²¹⁾	Rate	.053 ± .027

Table VI. Strange Particle Content of Neutrino Produced Dilepton Events

<u>Experiment</u>	<u>No. μ^-e^+ Events</u>	<u>No. Background μ^-e^+ Events</u>	<u>Corrected No. μ^-e^+ Events</u>	<u>No. of ν^0</u>	<u>$\nu^0/\text{CORR}\mu^-e^+$ Rate in %</u>
All Exp.	508	92	416	117	.28±.02
BNL-COL	249	31	218	58	.27±.03
Others	259	61	198	59	.30±.03

Table VII. Trilepton Production by Neutrinos and Antineutrinos

<u>Neutrino Beam</u>	$P_{\mu^{\pm}} \geq 4.5 \text{ GeV}/c$	
<u>EXPERIMENT</u>	<u>NO EVENTS</u>	<u>RATE $\frac{\mu^- \mu^- \mu^+}{\mu^-}$</u>
	$\nu \rightarrow \mu^- \mu^- \mu^+$	
CDHS ⁽²⁵⁾	76	$(3.0 \pm 0.6) \times 10^{-5}$
HPWFOR ⁽²⁶⁾	23	$(6.4 \pm 2.3) \times 10^{-5}$
<u>Antineutrino Beam</u>	$\bar{\nu} \rightarrow \mu^+ \mu^- \mu^+$	<u>RATE $\frac{\mu^+ \mu^- \mu^+}{\mu^+}$</u>
CDHS ⁽²⁷⁾	8	$(1.8 \pm 0.6) \times 10^{-5}$
		$\langle E_{\nu} \rangle = 57 \text{ GeV}$
		$(9 \pm 5) \times 10^{-5}$
		$E_{\nu} > 100 \text{ GeV}$

Table VIII. Same Sign Dilepton Production by Neutrinos and Antineutrinos

NEUTRINO PRODUCTION						
<u>Experiment</u>	<u>Beam</u>	<u>Events</u>	<u>Background</u>	<u>Cuts in GeV</u>	$(\mu^- \ell^- / \mu^- \ell^+)$ <u>Rate in %</u>	$\mu^- \ell^- / \mu^-$ <u>Rate in %</u>
CDHS ⁽³¹⁾	NBB	47 $\mu^- \mu^-$	30	$P_\mu > 4.5$	5±3	$\sim(3\pm 2)\times 10^{-4}$
CDHS ⁽³²⁾	WBB	290 $\mu^- \mu^-$	233	$P_\mu > 6.5$	4.1±2.3	$(3.4\pm 1.8)\times 10^{-5}$
		91 $\mu^- \mu^-$	71	$P_\mu > 10$	2.0±1.3	
HPWFOR ⁽³⁰⁾	QT,SSBT	38 $\mu^- \mu^-$	32	$P_\mu > 5$	6±5	
		18 $\mu^- \mu^-$	7.5	$P_\mu > 10$	12±5	
CFRRN ^(6c)	QT	12 $\mu^- \mu^-$	2-4	$P_\mu \gtrsim 9$	--	$(4-12)\times 10^{-4}$
BNL-COL	WBB	20 $\mu^- e^-$	9	$P_\mu > 10$ $2 < P_e < 20$	16±8	$\sim 3\times 10^{-4}$
ANTINEUTRINO PRODUCTION						
CDHS ⁽³¹⁾	NBB	9 $\mu^+ \mu^+$	5	$P_\mu > 4.5$	$\sim 5\pm 3$	
CDHS ⁽³²⁾	WBB	53 $\mu^+ \mu^+$	34	$P_\mu > 6.5$	4.2±2.3	$(4.3\pm 2.3)\times 10^{-5}$
		16 $\mu^+ \mu^+$	11	$P_\mu > 10$	2.2±1.7	